Mutations in *RD3* Are Associated with an Extremely Rare and Severe Form of Early Onset Retinal Dystrophy

Markus N. Preising,[1] *Nora Hausotter-Will,*[1] *Manuel C. Solbach,*[1] *Christoph Friedburg,*[1] *Franz Rüschendorf,*[2] *and Birgit Lorenz*[1]

Purpose. To identify the underlying mutation and describe the phenotype in a consanguineous Kurdish family with Leber's congenital amaurosis (LCA)/early onset severe retinal dystrophy (EOSRD).

Methods. Members of the index family were followed up to 22 years by ophthalmological examinations, including best corrected visual acuity (BCVA), Goldmann visual field (GVF), two-color-threshold perimetry (2CTP) and Ganzfeld electroretinogram (ERG), fundus photographs, fundus autofluorescence (FAF), and optical coherence tomography (OCT). After excluding seven of nine known LCA/EOSRD genes in the index patient, linkage analysis was performed in the family using a microarray followed by microsatellite fine mapping and direct sequencing of candidate genes. *RD3* was screened by direct sequencing of 85 independent patients with LCA/EOSRD presenting with a BCVA $\geq$ 1.0 LogMAR before the age of 2 years to assess the prevalence of *RD3* mutations in LCA/EOSRD. Since RD3 and RetGC1 have a functional relation, study authors screened for a modifying effect of *RD3* mutations in 17 independent patients with mutations in GUCY2D.

Results. BCVA was severely reduced from the earliest examinations (as early as 3 months), never exceeding 1.3 LogMAR. The disease presented as cone-rod dystrophy with dystrophic changes in the macula and bone spicules in the periphery on progression. Linkage analysis narrowed the region of interest towards the LCA12 locus. Direct sequencing of *RD3* revealed a homozygous nonsense mutation (c.180C > A) in all affected members tested. Screening of additional unrelated LCA/EOSRD patients revealed only polymorphisms in *RD3*.

Conclusions. This is the second family reported so far with mutations in *RD3*. Mutations in *RD3* are a very rare cause of LCA associated with an extremely severe form of retinal dystrophy. (*Invest Ophthalmol Vis Sci.* 2012;53:3463–3472) DOI:10.1167/iovs.12-9519

From the [1]Department of Ophthalmology, Laboratory of Molecular Ophthalmology, Justus-Liebig-University, Germany; and the [2]Max Delbrück Center for Molecular Medicine, Berlin-Buch, Germany.

Supported by DFG Lo457/5, Pro Retina Deutschland.

Submitted for publication January 17, 2012; revised March 22, 2012; accepted April 13, 2012.

Disclosure: **M.N. Preising**, None; **N. Hausotter-Will**, None; **M.C. Solbach**, None; **C. Friedburg**, None; **F. Rüschendorf**, None; **B. Lorenz**, None

Corresponding author: Markus N. Preising, Department of Ophthalmology, Laboratory of Molecular Ophthalmology, Justus Liebig University Gießen, Friedrichstrasse 18, 35392 Gießen, Germany; Tel: 0641-985 43837, Fax: 0641-985 43999, markus.preising@uniklinikum-giessen.de.

Leber's congenital amaurosis (LCA) is a genetically extremely heterogeneous disorder of the retina. Currently, 21 genes have been identified to cause various forms of retinal dystrophies with early onset presenting as cone dystrophies, cone rod dystrophies, and rod cone dystrophies (see Retina International Scientific News Disease Database, http://www.retina-international.org/sci-news/disloci.htm). Patients share a severe reduction of visual perception before the age of 2 years.[1] In the first decade of life, some visual function may be preserved at a low level. Fundus appearance varies from unremarkable to severe dystrophic features, depending on the underlying genetic cause.[1] LCA is progressive, but progression may be difficult to quantify due to severely reduced visual function prior to the ability of the patient to communicate.

Extremely severe phenotypes with very early visual loss of cone-rod dystrophy type have been reported in cases with pathogenic sequence changes in *AIPL1*, *CEP290*, *GUCY2D*, *RDH12*, and *RPGRIP*.[2–6] Mutations in these genes also are the most frequent causes of LCA worldwide. While homozygous or compound heterozygous sequence changes in *GUCY2D* cause very light or minimal morphological changes during childhood,[1] sequence changes of *AIPL1*, *CEP290*, *RDH12*, and *RPGRIP* present a phenotype with severe morphological changes of the fundus observable within the first months of age.[1,7,8] Mutations in other identified genes—e.g., *RD3, LCA5*, *CABP4*, *IMPDH1*, *IQCB1*, *KCNJ13*, *PDE6C*, *SPATA7*, *TULP1, ALMS1, CNGA3,* and *MYO7a*—contribute only sporadically to LCA, and the associated phenotypes vary considerably in severity and onset.[9–19]

After excluding the major genes of severe and early-onset retinal dystrophies, study authors linked the genetic cause in a Kurdish family with extremely severe early onset retinal dystrophy to the LCA12 locus on chromosome 1q32.1, and subsequently identified the underlying sequence change in *RD3*. The precise function of *RD3* is still unknown. It is believed to be able to suppress retinal membrane guanylate cyclase activity, and potentially plays an important role in retinal maturation.[20]

This is the second family reported so far worldwide. Evaluation of other patients with early onset severe retinal degenerations revealed only polymorphisms in the heterozygous state in *RD3*.

Methods

Patients

Four siblings (0659.1, 0659.2, 0659.4, 0659.5), affected with Leber's congenital amaurosis from an extended Kurdish family (Fig. 1A), were seen repeatedly in the Department of Ophthalmology of the University Medical Center Giessen between 1989 and 2010 at ages ranging from 4 months to 22 years. Three additional relatives were affected and two of

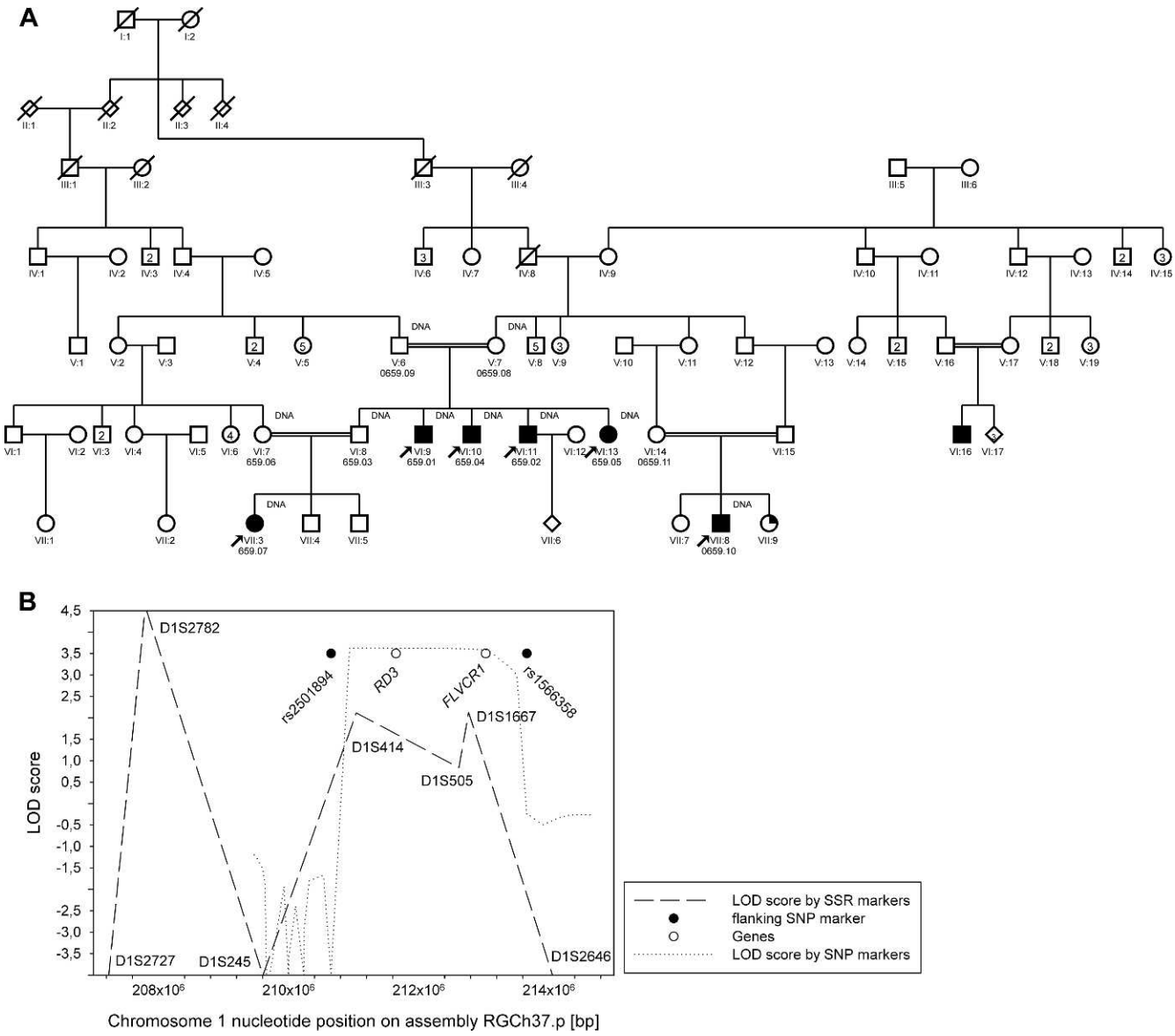

Figure 1. Pedigree and linkage analysis in family 0659. (**A**) Pedigree of family 0659. ○ females, □ males, ◇ unknown sex, ◔ Osteogenesis imperfecta, *open symbols* indicate unaffected individuals, *closed symbols* indicate affected individuals, *stricken symbols* indicate deceased individuals, *arrows* indicate examined individuals, *double marriage lines* indicate consanguinity. (**B**) Plot of lod scores calculated from single nucleotide polymorphism (SNP) marker typing and short sequence repeat (SSR) marker typing. Positions of candidate genes are indicated by *open circles*. Positions of flanking SNP markers are indicated by *solid circles*. SSR markers associated with the corresponding data points.

these (0659.07 and 0659.10) were seen in the department at ages 3 months to 10 years.

A reference group of patients was chosen from the study authors' database of patients with early-onset severe retinal dystrophy (EOSRD) and a best-corrected visual acuity (BCVA) of 0.1 and less (1.0 LogMAR) before the age of 2 years to evaluate the frequency of *RD3* sequence changes.

To evaluate a modifier effect of RD3 on RetGC1 function, patients carrying disease causing sequence changes in *GUCY2D* were included in the mutation screen.

The study was approved by the Institutional Review Board of the Medical Faculty of the Justus-Liebig University Giessen (Application No. 149/07) and adhered to the tenets of the Declaration of Helsinki.

Clinical Examination

Visual acuities were obtained with best correction using Teller acuity cards (TAC), LH cards, or orientation of the letter E. Further ophthalmic examination included funduscopy and color vision testing using the Farnsworth or Lanthony desaturated panel D 15 test. Pupil responses were tested.

Perimetry. *Kinetic Perimetry.* Kinetic photopic visual fields were measured with a Goldmann perimeter (Haag-Streit, Bern, Switzerland) using 2 targets (V/4e, III/4e).

Two-Color Threshold Perimetry. Two-color threshold perimetry (2CTP) was performed under scotopic and photopic conditions to assess the spatial distribution of rod and cone mediated function. A modified Humphrey-Field-Analyzer (HFA, model 640 modified by F. Fitzke; Institute of Ophthalmology, London, UK) was used as reported previously.[21]

Electroretinography. Full-field electroretinograms (ERGs) were recorded with DTL electrodes with a Nicolet Spirit and a Ganzfeld bowl (Nicolet, Madison, WI) following the guidelines of the International Society for Clinical Electrophysiology in Vision (ISCEV).[22] Artefacts caused by nystagmus were rejected.

Imaging. Fundus pictures were taken using a standard Zeiss fundus camera (FF450; Carl Zeiss Meditec, Jena, Germany).

Fundus autofluorescence (FAF) was recorded using a confocal scanning laser ophthalmoscope module (Heidelberg Retina Angiograph [HRA] module of a Spectralis Unit; Heidelberg Engineering, Heidelberg, Germany). A detailed description is given elsewhere.[23] The FAF signal was amplified by an automatic software tool of the Spectralis Unit.

Optical coherence tomography (OCT) was performed using the same device with the second laser. The fovea and areas of the posterior pole were scanned.

Molecular Genetics

Patient DNA was screened for sequence changes in retinal guanylate cyclase (*GUCY2D*), RPE-specific 65 kDa (*RPE65*) protein, lecithin retinol acyltransferase (*LRAT)*, aryl-hydrocarbon-interacting protein-like 1 (*AIPL1*), cone-rod homeobox (*CRX*) protein, human crumbs homolog 1 (*CRB1*), and for the p.C998X (c.2991+1655A > G) sequence change in centrosomal protein 290kDa (*CEP290*) by PCR-SSCP employing methods reported previously.[1]

Linkage studies were initiated submitting the core family of four affected siblings, the unaffected brother and the parents, to single nucleotide polymorphism (SNP)-genotyping using a microarray (Affymetrix Mapping 50k Xba 240; Affymetrix, High Wycombe, UK). The microarray data were processed using ALOHOMORA[24] and parametric linkage analysis was performed in MERLIN[25] (Fig. 1B).

To narrow down the area of linkage, short sequence repeat (SSR) markers (Fig. 1B) were taken from the UniSTS and dbSNP database at the National Center for Biotechnology Information (NCBI) and from the Ensemble Genome Browser. SSR markers were typed by polymerase chain reaction (PCR) and capillary electrophoresis on an automated analyzer (QIAxcell System; Qiagen, Hilden, Germany).

Data were transferred to the pedigree using a software database (Cyrillic 2.1.3; FamilyGenetix Inc., Oxford, UK) and parametric linkage analysis was performed in MERLIN.[25]

For direct sequencing, two primer pairs covering coding and flanking intronic sequences of *RD3* (*RD3*-2: forward: CTCTCCTGGGTCCCAGCTCT, reverse: AGCCACCTTTCCTGGAGCCT – 466 bp; *RD3*-3: forward: TGAAGCAGTAGCAGCGTGGG; reverse: CTGCAGAAGGCTCCGCTTCT – 496 bp) were designed from GenBank record NG_013,042.1 using analysis software (Vector NTI Advance 11; Invitrogen, Darmstadt, Germany). Two fragments of *RD3* were amplified by PCR from patient DNA and submitted to Sanger sequencing at a commercial sequencing company (Seqlab, Göttingen). Sequence data were compared with the wildtype sequence of *RD3* GenBank record (NG_013,042.1) using GENtle software (Magnus Manske).

Results

Clinical Examination

Clinical data of the six patients examined every 2 or 3 years are summarized in Table 1. BCVA was never better than 0.08 (LogMAR < 1.12) by TAC and 0.05 (LogMAR 1.3) by LH cards or E signs. BCVA declined over time, finally resulting in light perception only (Fig. 2A). Pupillary reactions were present at all times, but sluggish in the index patient at his first examination at 4 months. All patients reported glare sensitivity and some improvement with longpass filters (Clarlet F580 and F90; Carl Zeiss, Jena, Germany), or plastic lenses (ORMA RT70; Essilor, Hanau, Germany).

Initial refraction was hypermetropic and changed to myopic in the disease course (Fig. 2B).

Imaging. Patients were seen as early as 4 months (median initial funduscopy). Funduscopy before the age of 2 years was unremarkable. From approximately 2 years on, attenuated vessels and macular changes were noted progressing from loss of macular wall reflex to a bull's-eye lesion with central yellow pigment in childhood (Fig. 3A). Fundus photographs obtained in all but the youngest patients (see Table 1) allowed a side-to-side analysis of these changes at the end of the first (patient 0659.07, see Fig. 3A) and second decade of life (patients 0659.01, 0659.02, 0659.04, 0659.05, see Figs. 3B–D). In adolescence, these macular changes resolved into yellow spots (Fig. 3B). At the beginning of the third decade of life, the peripheral fundus demonstrated a hammer beaten appearance and later bone spicules (Figs. 3C, 3D).

Meaningful FAF could only be obtained in patient 0659.07. At age 7 years, it was strongly reduced within the macula, diffusely increased in a broad ring around that area, and fading out to the periphery (Fig. 4).

OCT recordings of the macular area could be obtained at the age of 10 years (patient 0659.07, Fig. 5B) and at the turn of the second into the third decade of life (patients 0659.02 and 0659.04, Fig. 5C). Due to severe nystagmus, all recordings were difficult to obtain and to reproduce. At a younger age, the stratification of the retina was disorganized in all layers. The connecting cilia (CC), the photoreceptor outer segments (POS), and the retinal pigment epithelium (RPE) layers were absent at that age (Fig. 5A, white arrows). The photoreceptor inner segments (PIS) and the external limiting membrane (ELM) were preserved though irregularly displaced (Fig. 5, black arrows). The thickness of the PIS and the outer nuclear layer (ONL) were reduced as well as the subsequent neuronal layers (outer plexiform layer [OPL]; inner nuclear layer [INL]; inner plexiform layer [IPL]) (Fig. 5, black asterisk). The ganglion cell layer (GCL) (Fig. 5, white asterisk) was present, although abnormal in appearance as well as the nerve fibre layer (NFL) that was severely disorganized. At later ages, the ELM was preserved but severely displaced and the PIS and ONL layers gained more space. The OPL, INL, and IPL were severely reduced in thickness and stratification was hard to distinguish. The GCL and the NFL were also diminished. The reproduction of the different layers was suboptimal at all ages due to the recording conditions under the heavy nystagmus.

Visual Field and Sensitivity. Goldmann visual fields (GVF) could be measured in five patients and as early as 5–7 years. Even then, it was severely constricted to 20° and less for the Goldmann III/4e target. At later ages, recognition of that target failed and only testing with V/4 revealed residual central retinal light perception.

Retinal sensitivity was sufficiently preserved in three patients to be measured by 2CTP. Scotopic sensitivity loss was in the range of 5 log units. The tests revealed massive sensitivity loss for blue stimuli under scotopic and photopic conditions in the three patients tested (Table 1). Residual sensitivity mediated presumably by cones (red stimulus, scotopically matched blue stimulus too dim) could be obtained in the eldest patient under scotopic conditions. Interindividual variability was too large to draw any conclusions as to progression with age.

Electrophysiology. ERGs were recorded in four patients between the age of 5 and 10 years. All were below noise level (Table 1). VEPs were recorded at 2 years in one patient, and were below noise level, too.

Genetic Investigations

Seven individuals from the core family (see Fig. 1A) were genotyped for SNPs using the microarray mentioned previously (Affymetrix Mapping 50k Xba 240, Affymetrix). After processing the data in ALOHOMORA and MERLIN, a genome wide LOD score map was built indicating a maximum LOD score of 3.627 at 1q31-32 between nucleotide 209,473,694 and

Table 1. Phenotype Data Obtained in Six Affected with a Homozygous *RD3* Mutation

Patient	0659.04	0659.01	0659.02	0659.05	0659.07	0659.10
Nystagmus	Congenital	Congenital	Congenital	Congenital	Congenital	Congenital
Glare sensitivity	⊕⊕⊕	⊕⊕⊕	⊕⊕⊕	⊕⊕⊕	⊕⊕⊕	⊕⊕⊕
Color vision	↓	↓	↓	↓	↓	np
Pupillary reaction	**22 years**: ⊕	**4 months**: ⊕ **20 years**: ⊕⊕⊕	**19 years**: ⊕	**17 years**: ⊕	**10 years**: ⊕	**4 years**: ⊕ bright light
Refraction/visual acuity	**3 years**: RE +11.25/−3.5/5° LE +11.25/−3.5/172° **5 years**: RE +11.0/−3.5/8° LE +11.0/−3.25/10° TAC : RE 0.07 LE 0.05 **7 years**: RE +7.250/−4.5/19° = 0.034 LE +7.25/−3.5/170° = 0.036 bin: D: 0.04 C: <0.1 **11 years**: RE +10.0/−3.5/20 = 0.008 LE incomplete LP **14 years**: o.u. incomplete LP **22 years**: o.u. LP	**8 months**: follows light, no fixation **2 years**: RE +4.5/−3.0/20° LE +5.25/−3.75/170° **5 years**: RE +4.5/−3.0/15° LE +5,25/−3.75/176° = 0.04 bin = 0.04 **8 years**: RE +4.0/−3.0/12° = 0.1/30 LE +4.5/−3.25/165° = 0.008 **10 years**: RE np LE 0.006 **20 years**: o.u. LP	**1 year**: uncertain fixation **1.5 years**: RE +10.5/−3.0/10° = 0.05 LE +9.5/−1.5/176° = 0.0125 bin 0.03 **4.5 years**: RE +6.5/−3.0/0° = 0.02 LE +7.5/−2.75/176° = 0.04 bin = 0.06 **7 years**: RE +5.75/−3.75/9° LE +6.5/−2.5/171° o.u. 0.05, bin 0.08 **10 years**: RE +5.75/−3.5/10° LE +6.75/−2.5/162° = o.u. 0.05 **11 years**: RE +5.5/−2.75/12° = LP, LE +6/−2.25/165° = 0.032 **14 years**: o.u. LP **19 years**: RE +1.0/−3.0/29°, LE +0,75/−2.75/154° o.u. LP	**1 year**: o.u. +5.5, defense reaction on cover **2.5 years**: RE +8.5/−3.5/178° LE +8.5/−3.5/12° fixation **5 years**: RE +6.5/−4.5/14° LE +6.5/−3.5/5° o.u. 0.04, bin: 0.05 **7 years**: RE +6,5/−4,5/14° LE +6,5/−3.5/5° LH o.u. 0.04, bin: 0.05 **9 years**: RE +6.74/−4.0/8° LE +6.0/−5.75/168° o.u. 0.04 **10 years**: RE +6.5/−4.0/7° LE +6.0/−3.75/171° o.u. 0.04 **17 years**: RE +3.25/−4.0/2° <0.008, CF LE +1.25/−4.0/170° = 0.008	**3 months**: o.u. +5.5 sph, no reaction to light **7 months**: o.u. +7.0/−1.0/0°, TAC: bin 0,03, fixation **14 months**: TAC bin 0.034 **19 months**: TAC RE: 0,034, LE: 0,014 **2 years**: RE +5.5/−1.5/12° = 0.05 TAC LE +5.75/−2.25/0° = 0.025 TAC **3 years**: RE +5.5/−1.5/12° LE +5.75/−2.25/0° o.u. 0.08 TAC **6 years**: RA +2.5/−1.5/16° = 0,05 LA +2.5/−1.5/170° = 0,01 **8 years**: RE +1.5/−3.75/8° LE +1.25/−3.5/158° bin 0.01 ETDRS **10 years**: o.u. LP	**1 year**: TAC: no cooperation, fixates desk light **4 years**: RE +4.0/−1.50/15° LE +4.5/−1.75/152° observes room, no visual contact to persons
Visual field	**11 years**: Goldmann III/4 nr	**8 years**: RE 30°, LE 30° - 20° - 15° - 5° **10 years**: Goldmann III/4 nr	**7 years**: np **10 years**: Goldmann RE III/4 nr, V/4: 10° - 22° - 5° - 5° LE III/4: 8° - 10° - 10° - 10°	**5 years**: Goldmann RE 20 - 25°, LE 25 – 30° **7 years**: Goldmann III/4 RE 18°-25°-15°-20° LE 15°-20°-60°-50° **10 years**: Goldmann III/4 o.u. 20° V/4 o.u. 40° - 50° **17 years**: Goldmann III/4 o.u. nr, V/4 RE 20 - 40° LE 40° – 50°	**8 years**: Goldmann: minimal central residues	np

Table 1. Continued

Patient	0659.04	0659.01	0659.02	0659.05	0659.07	0659.10
Fundus/FAF	**3 years**: No MWR, bull's eye macula, ONH and periphery regular **5 years**: ONH pale, attenuated vessels, maculopathy, peripheral flecks, drusen-like flecks **7 years**: ONH regular, macula granular depigmentation **11 years**: ONH peripheral degeneration, macula yellow-white deposits attenuated vessels **14 years**: ONH pale, macula yellow-white **22 years**: ONH waxy, intensive macular depigmentation into mid-periphery, bone spicules attenuated vessels (Fig. 3D)	**4 years**: ONH, macula, and periphery regular **5 years**: ONH regular, pigmented changes in macula attenuated vessels, periphery regular **8 years**: ONH pale, pigmented changes in macula like vitelliform maculopathy, periphery regular **10 years**: ONH ↓ fibers, yellow-white spots in fovea, attenuated vessels **15 years**: ONH regular, attenuated vessels, macula pale with pigment irregularities periphery regular **20 years**: ONH pale, attenuated vessels, macula yellowish, white deposits	**4.5 years**: ONH like Hyperopia, macula implies vitelliform maculopathy, periphery regular **7 years**: ONH pale, vitelliform pigment in fovea, periphery unremarkable **10 years**: ONH regular, vessels attenuated, macula and mid-periphery dystrophic signs **19 years**: ONH atrophic, macular degeneration, vessels attenuated, pigment changes in fundus FAF: mottled, ↓	**2.5 years**: ONH regular, nasally blurred, attenuated vessels, periphery regular, hypopigmented, macula de- and hyperpigmented, vitelliform-like **7 years**: MWR abnormal, pigment irregularities **9 years**: ONH pale, irregular macular reflexes **17 years**: ONH pale, regular, macular depigmentations, de- and hyperpigmentations in periphery, vessels attenuated (Fig. 3B)	**7 months**: macula, ONH, periphery regular **2 years**: ONH and periphery regular, MWR faint **3 years**: attenuated vessels, macula brightened with dark halo **5 years**: RE +2.75/−1.5/10° = 0.1060, LE +3.0/−2.0/170° = 0.0533 (LH) **6 years**: ONH regular, very attenuated vessels, macula brightened with dark halo **8 years**: ONH pale, macular surface irregular, peripheral retinal surface hammer-beaten, pigment irregularities **10 years**: see Fig. 3A, no change from 8 years.	**1 year**: unremarkable periphery, macula with scar, ONH regular **4 years**: macular degeneration, ONH regular, vessels unremarkable, pigmentation uneven, FAF ↓ in macula
Electrophysiology neurophthalmology	**5 years**: ERG bt		**10 years**: ERG bt	**9 years**: ERG: bt	**2 years**: VEP non reproducible **8 years**: ERG bt	**1 year**: OKN ⊕
OCT	**22 years**: retinal thickness ↓, irregular reflexes over RPE, see Fig. 5		**19 years**: retinal thickness ↓, irregular reflexes over RPE, see Fig. 5		**10 years**: retinal thickness ↓, loss of stratification especially in the outer retina, see Fig. 5	
2CTP		**20 years**: RA: bt LA: scot.: residual responses to red stimulus		**17 years**: LE: massive loss of scot. sensitivity, phot. blue bt	**10 years**: RE: scot. bt	
Comments	Edge filter glasses (Clarlet F580 and F90) reduce glare sensitivity	Edge filter glasses (Clarlet F580 and F90) reduce glare sensitivity	Edge filter glasses (Clarlet F580 and F90) reduce glare sensitivity	Edge filter glasses (Clarlet F580 and F90) reduce glare sensitivity	Edge filter glasses (Clarlet F580 and F90) reduce glare sensitivity	Edge filter glasses (ORMA RT70) reduce glare sensitivity

Visual fields are represented by their four-digit code of inferior - temporal - superior - nasal visual field maxima. Other values represent a range of maximal visual field. Refraction is given as three data coda of refraction/cylinder/torsion. Abbreviations: ⊕, present; ⊕⊕, strong; ⊕⊕⊕, severe; ↓, reduced; ↑, increased; Ø, absent; RE, right eye; LE, left eye; o.u., both eyes; HM, hand movement; LP, light projection; bt, below threshold; np, not possible; nr, not recognized; scot., scotopic; phot., photopic; D, Distance; ONH, optic nerve head; MWR, macular wall reflex; LH, LH-cards; TAC, Teller Acuity cards.

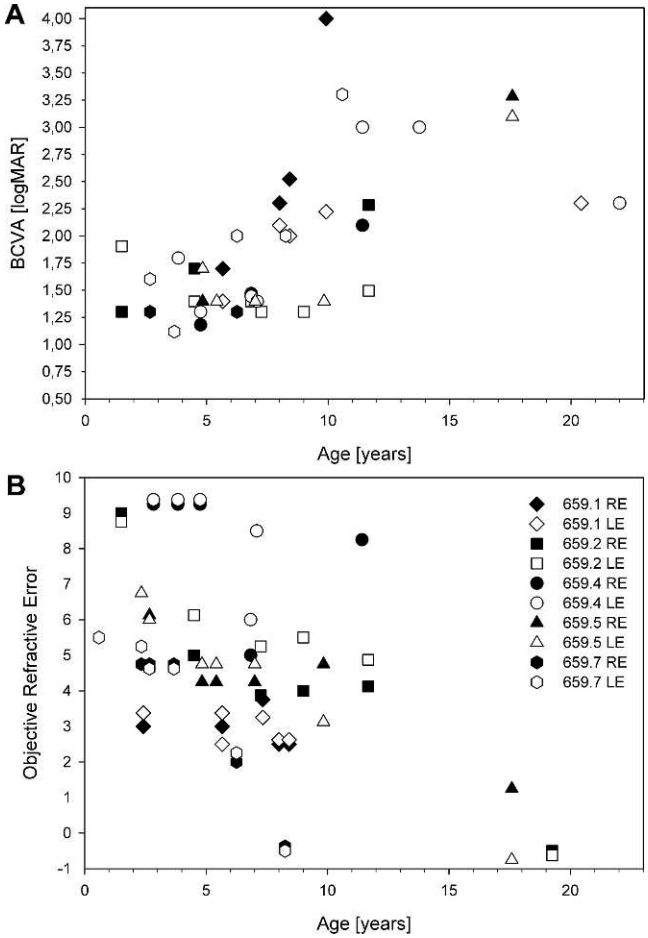

Figure 2. Best corrected visual acuity. (**A**) Objective refractive error. (**B**) Five of six patients. *Open symbols* denote data from the right eye; *closed symbols* denote data from the left eye of each patient. Counting fingers (CF, LogMAR 1.85), movement (HM, LogMAR 2.28), and light perception (LP, LogMAR 3.3) were digitalized according to Schulze-Bonsel et al.[38]

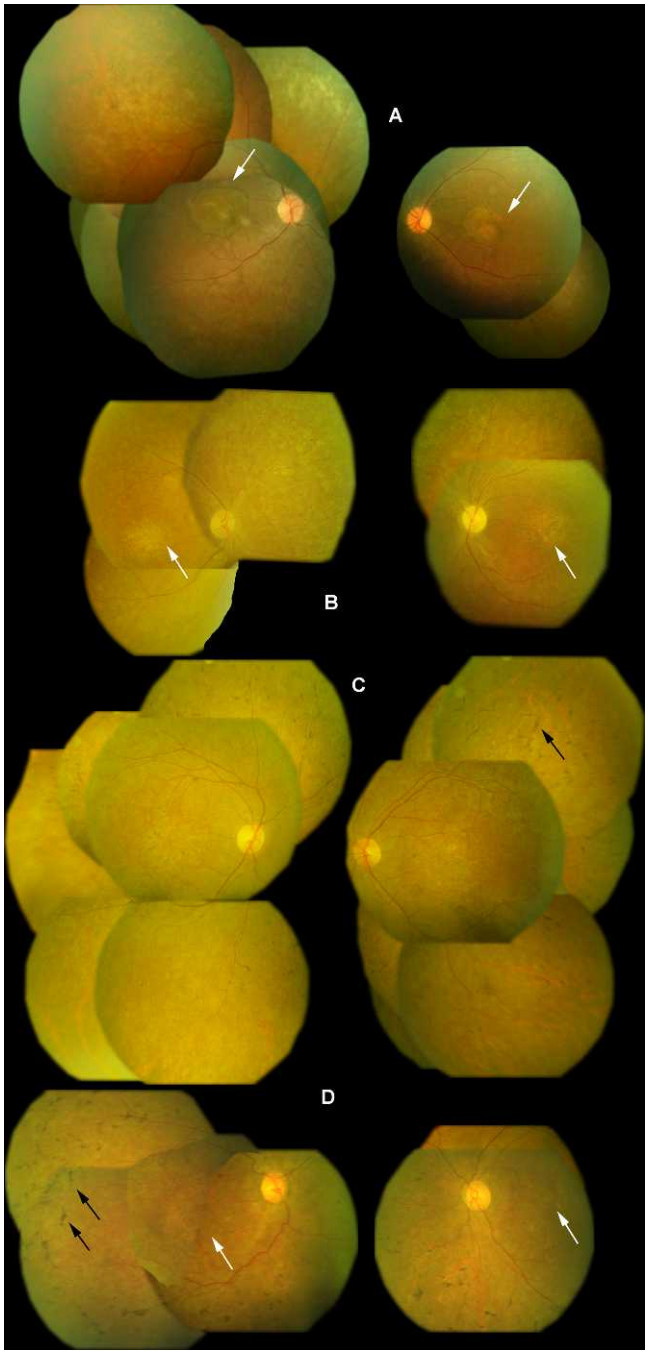

Figure 3. Fundus photographs of patients at different ages. (**A**) 0659.07 at 10 years. (**B**) 0659.05 at 17 years. (**C**) 0659.02 at 19 years. (**D**) 0659.04 at 22 years. *Black arrows* indicate bone spicules developing on disease progression, *white arrows* indicate bull's-eye maculopathy developing with yellow deposits into yellow spots, and finally dissolute.

214,664,986 (assembly RGCh37.p5). Study authors further typed short sequence repeat markers within and flanking this region to narrow down the region of interest (see Fig. 1B). Recombination events flanking the LCA12 locus were identified.

Consequently, study authors directly sequenced the *RD3* gene in the index case and identified a homozygous nonsense mutation in codon 60 (p.Y60X, c.180C > A). This mutation could be shown in the homozygous state in the DNA of all available affected members of the family. All parents of the patients carried the mutation in the heterozygous state.

In addition, 85 patients were screened for sequence changes in *RD3*. Among these, 44 patients were diagnosed with LCA; 12 patients with early onset cone or cone rod dystrophies including 3 index cases of dominant inheritance; and 29 patients with EOSRD (Table 2). Among these patients, six sequence changes were identified in 32 patients (p.R47C [c.141C > T], p.G57V [c.170G > T], c.296+28G > A, c.297-86A > T, c.297-124G > A, c.486C > T). The most frequent sequence changes were c.297-86A > T (21 patients, 4 homozygous); c.297-124G > A (10 patients); and p.R47C (4 patients). p.R47C and p.G57V were reported elsewhere, with p.R47C being regarded as benign sequence change and p.G57V as a sequence change of uncertain pathogenicity. p.G57V was identified in the heterozygous state in a Scandinavian girl presenting with visual problems at the age of 6 years making this sequence change an unlikely cause of the disease.[10]

Seventeen of these patients carried *GUCY2D* sequence changes. Even though no pathogenic mutation was identified, nine of these patients carried the c.297-86A > T or c.297-124G > A mutation in *RD3*.

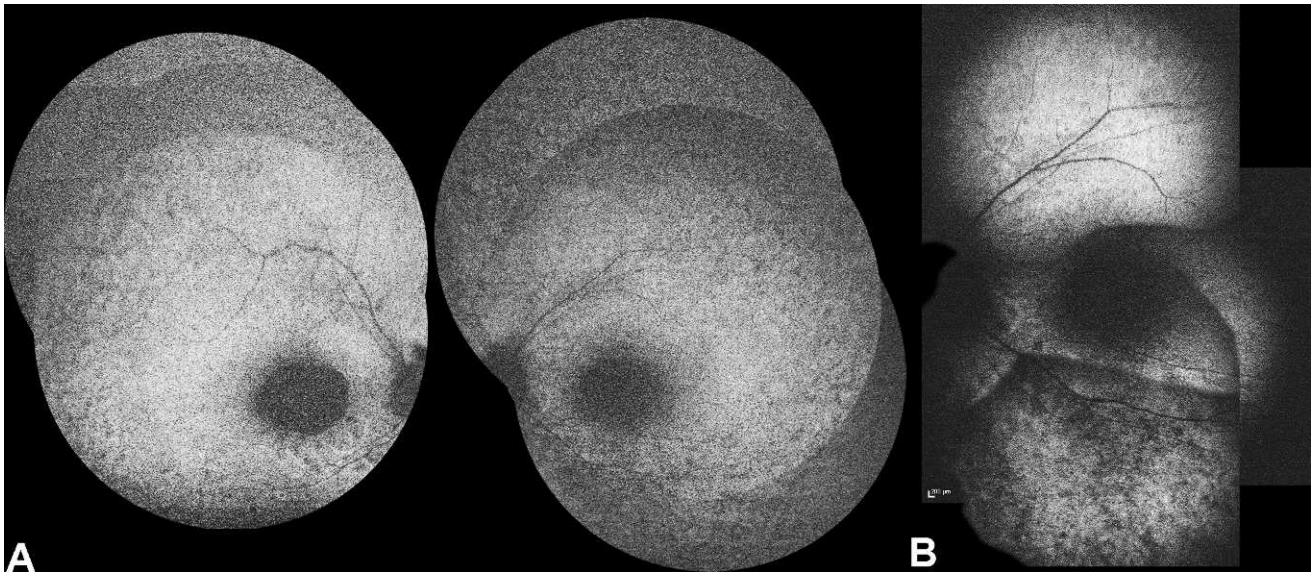

Figure 4. FAF recoding from patient 0659.07 at age 7 years. (**A**) 50°-wide field recording of the right and left eye. (**B**) 30°-field recording of the left eye. Note absent FAF in macula and the increased FAF in the surrounding retina fading out to the periphery.

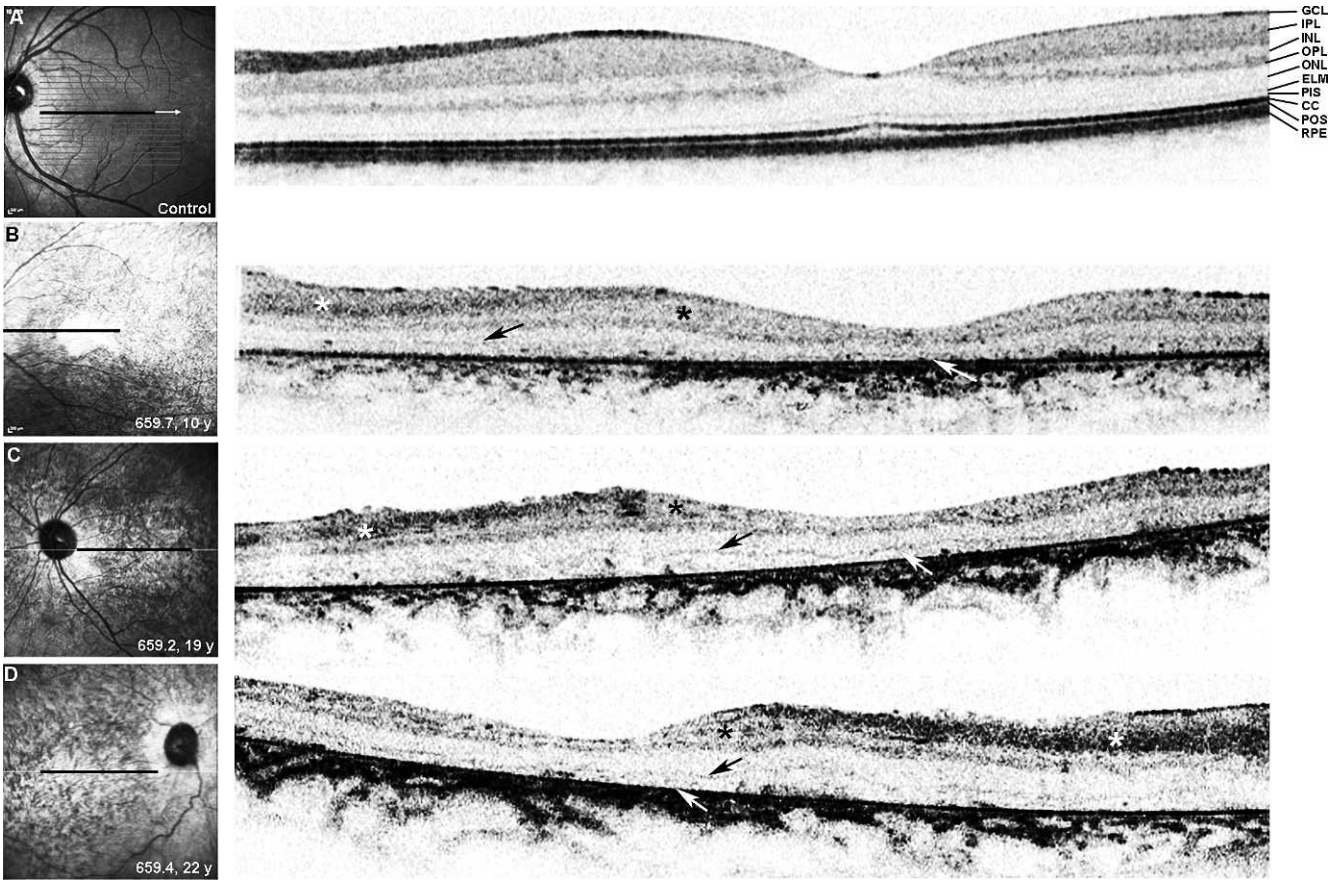

Figure 5. Optical coherence tomography (OCT) recording. (**A**) Normal control individual. (**B**) Patient 0659.07 at 10 years. (**C**) Patient 659.02 at 19 years. (**D**) Patient 0659.04 at 22 years. *Black arrows* indicate the ELM to locate the disorganized photoreceptor layers, *white arrows* indicate the position of the RPE layer. *White asterisks* indicate the GCL and *black asterisks* indicate the layers covering the neuronal cells (OPL, INL, IPL). Note the missing CC, POS, and RPE, the reduced thickness of the ONL, and the neuronal cell layers in 0659.07. Reduced stratification of layers may be an artifact of the lower resolution of the recording caused by the nystagmus, but also indicates intraretinal disorganization with progression.

Table 2. Summary of Patients Screened for Mutations in *RD3*

Disease	Cases screened	*RD3* polymorphisms	GUCY2D mutations	GUCY2D + *RD3*
LCA	44	4	10	3
COD/CRD	12	0	0	3*
EOSRD	29	10	0	1
Sum	85	14	10	7

* Patients with autosomal dominant inheritance.

Discussion

This study is the second to identify a family with LCA/EOSRD caused by a sequence change in *RD3*. The homozygous nonsense mutation p.Y60X (c.180C > A) introduces a premature stop codon before the final intron. The truncation abolishes approximately two-thirds of the gene product predicting nonsense-mediated decay to remove the mRNA before translation.

The mouse model *RD3* is a classical naturally occurring animal model of inherited retinal degeneration in mice[26,27] occurring between postnatal weeks 2 and 3, starting with slimming of the ONL and the PIS, CC, POS layers and progressing into complete loss of all photoreceptors by post natal weeks 7 to 8. At that time, ERG responses were already below noise level. The ultrastructural and functional features are accompanied by narrow vessels on funduscopy and an increasing number of hypopigmented spots at postnatal week 21, progressing into areas of hypo- and hyperpigmentation by postnatal week 40.

The naturally occurring dog model was reported much earlier as rod cone dystrophy 2 (*RCD2*) in collies.[28,29] Similar to mice, these dogs are affected very early. Rod components of the ERG response get lost early and cone components remain normal to slightly reduced in amplitude and latency in the beginning of progression.[29] By 7 weeks, rods are almost completely lost. At the same time, the cones show club-shaped inner and disorganized outer segments. Compared with the outer plexiform and ganglion cell layer, the photoreceptor layer was much more affected.[29] Levels of cGMP were increased.[28]

The gene underlying the mouse model *RD3* was identified in 2006[10] and its involvement in *RCD2* has been shown very recently.[30] Identification of the mouse model *RD3* gene directly let to the identification of sequence changes in the human *RD3* gene as the underlying cause in an Indian family with LCA.[10] The patients presented with poor vision from birth, nystagmus, and atrophic lesions in the macular area. The periphery showed bone spicules. The underlying sequence change was identified as a homozygous splice mutation introducing a premature stop codon at position 100 abolishing almost 50% of the gene product.

In this study, we followed six affected patients from one family between the age of 3 months and 22 years. Based on available data, this is the second family reported so far. The phenotype resembles well those seen in both animal models. BCVA and electrophysiology indicated a global and severe loss of visual function from the earliest ages onwards. OCT revealed disorganization of all retinal layers including the GCL and NFL at later stages. This is comparable to the histological data from the animal models.[26,31] The ELM was preserved though dislocated possibly reflecting remaining PIS, as it was shown in the *RCD2* collies.[31] Preservation of the PIS, ELM, and ONL may provide some chance of successful application of optogenetics.[32–34] However, significant changes in the GCL and NFL may represent serious limitations to success. Reduced thickness of the OPL, INL, and IPL indicates incomplete preservation of the neuronal layers. Whether this was present from birth—and thus preventing the development of structures necessary for the formation of the visual cortex, thus arguing against a useful application of optogenetics—or whether it is acquired over time cannot be deduced from the presented data.

The disease involves both rods and cones indicated by night blindness, the narrowing visual fields, and the severely impaired visual acuity, the nonrecordable ERG, and nystagmus. Glare sensitivity was reported as a major problem and was successfully diminished by blue light–blocking longpass filters.

The gene product of *RD3* has been described to interact with RetGC1 and RetGC2.[20,35] Colocalization of RetGC1 and RetGC2 has been shown by immunohistochemistry in the ER and endosomal vesicles in mice.[10,35] RD3 suppresses the guanylate cyclase activity of RetGC in rods and cones in the absence of GCAP, and inhibits RetGC function at low Ca^{2+}-concentration. It antagonizes GCAP function but does not change Ca^{2+}-sensitivity of GCAP regulation of RetGC.[20] From these data, a chaperone function of RD3 on RetGC has been predicted, which would explain reduced RetGC contents in the outer segments of the mouse model *RD3*.[35] RD3 suppresses cGMP synthesis at basic cGMP levels.[20] And, indeed, increased cGMP levels are a common feature of several mouse models and were shown in the initial studies of the mouse model *RD3* many years ago.[28] In addition, the impaired posttranslational intracellular transport of RetGC1 displaces the cGMP production from the outer to the inner segment, impairing dissimilating enzymatic activity on cGMP by phosphodiesterase thus increasing the cGMP level in the photoreceptors.

The visual function of LCA1 (mutations of *GUCY2D*) and LCA12 (mutations in *RD3*) patients should therefore be comparably reduced, depending on the dose of functional loss associated with the individual sequence changes carried by a patient. Severe loss of visual function at birth is the prominent feature of *GUCY2D* sequence changes.[1] The nonsense mutation in *RD3* in this study predicts a complete loss of function of RD3, resulting in uncontrolled basal activity and impaired intracellular transport of RetGC1. The resulting visual function loss is comparably reduced to patients with *GUCY2D* sequence changes and in line with the data obtained from the LCA12 family reported previously.[10] In contrast to *GUCY2D* sequence changes a severe and early disorganization of the PIS, CC, and POS layer is present together with the loss of function by *RD3* sequence changes. This resembles the morphological data form the mouse model *RD3* and *RCD2* collies.[26,31] The PIS appeared thickened but preserved. The reason for this early degenerative process in LCA12, compared with the less-pronounced early degeneration in LCA1, may result from increased cGMP concentrations by the basal activity of RetGC1 in the PIS and reduced amounts of RetGC1 in the POS that result from loss of RD3 function in LCA12. In LCA1, RetGC1 function is lost, impairing the production of cGMP, which is less deleterious than an excess of cGMP. In addition, *GUCY2D* mutations may not impair the synthesis of RetGC1 molecules,

but only their activity thus providing RetGC1 molecules to stabilize the POS.

Study authors screened other patients with very early and severe loss of visual function and associated retinal degeneration in order to test for a possible involvement of *RD3*. Among these patients, only single heterozygous conditions with either missense mutations or intronic polymorphisms were identified. This is in line with previous studies screening for sequence changes in *RD3*.[10,36,37]

Finally, study authors sought to identify a possible modifying activity of *RD3* sequence changes in patients carrying *GUCY2D* sequence changes. Study authors screened 17 index patients with autosomal recessive and autosomal dominant *GUCY2D* sequence changes and identified almost the same set of benign sequence changes as in the retinal degeneration panel, thus indicating that *RD3* does not play a role in the etiology in this study's set of LCA1 patients.

The findings of this study indicate that sequence changes in *RD3* are a very rare cause of LCA and if present, are associated with a very severe phenotype. The most prominent morphological feature on OCT is the thickened PIS layer and the well visible ELM.

Online Web Resources

Retina International Scientific News Disease Database: http://www.retina-international.org/sci-news/disloci.htm Retina International.

National Center of Biotechnology Information (NCBI), http://www.ncbi.nlm.nih.gov/ National Institutes of Health, Bethesda, MD, USA.

Integrating Markers and Maps (UniSTS): http://www.ncbi.nlm.nih.gov/unists National Institutes of Health.

Nucleotide: http://www.ncbi.nlm.nih.gov/nuccore National Institutes of Health.

Short Genetic Markers and Maps (dbSNP): http://www.ncbi.nlm.nih.gov/snp National Institutes of Health.

Ensembl Genome Browser: http://www.ensembl.org/index.html European Bioinformatics Institute of the European Molecular Biology Laboratory (EMBL–EBI) and the Wellcome Trust Sanger Institute.

GENtle Software: http://gentle.magnusmanske.de/ Magnus Manske, University of Cologne, Germany.

Splice Sequence Finder: http://www.umd.be/HSF/ C. Béroud INSERM U827.

References

1. Preising MN, Paunescu K, Friedburg C, Lorenz B. [Genetic and clinical heterogeneity in LCA patients. The end of uniformity]. *Ophthalmologe*. 2007;104:490–498.
2. Perrault I, Rozet JM, Calvas P, et al. Retinal-specific guanylate cyclase gene mutations in Leber's congenital amaurosis. *Nat Genet*. 1996;14:461–464.
3. Sohocki MM, Bowne SJ, Sullivan LS, et al. Mutations in a new photoreceptor-pineal gene on 17p cause Leber congenital amaurosis. *Nat Genet*. 2000;24:79–83.
4. Janecke AR, Thompson DA, Utermann G, et al. Mutations in RDH12 encoding a photoreceptor cell retinol dehydrogenase cause childhood-onset severe retinal dystrophy. *Nat Genet*. 2004;36:850–854.
5. den Hollander AI, Koenekoop RK, Yzer S, et al. Mutations in the CEP290 (NPHP6) gene are a frequent cause of Leber congenital amaurosis. *Am J Hum Genet*. 2006;79:556–561.
6. Dryja TP, Adams SM, Grimsby JL, et al. Null RPGRIP1 alleles in patients with Leber congenital amaurosis. *Am J Hum Genet*. 2001;68:1295–1298.
7. Testa F, Surace EM, Rossi S, et al. Evaluation of Italian patients with Leber congenital amaurosis due to AIPL1 mutations highlights the potential applicability of gene therapy. *Invest Ophthalmol Vis Sci*. 2011;.
8. Pasadhika S, Fishman GA, Stone EM, et al. Differential macular morphology in patients with RPE65-, CEP290-, GUCY2D-, and AIPL1-related Leber congenital amaurosis. *Invest Ophthalmol Vis Sci*. 2010;51:2608–2614.
9. Littink KW, van Genderen MM, Collin RW, et al. A novel homozygous nonsense mutation in CABP4 causes congenital cone-rod synaptic disorder. *Invest Ophthalmol Vis Sci*. 2009;50:2344–2350.
10. Friedman JS, Chang B, Kannabiran C, et al. Premature truncation of a novel protein, RD3, exhibiting subnuclear localization is associated with retinal degeneration. *Am J Hum Genet*. 2006;79:1059–1070.
11. den Hollander AI, Koenekoop RK, Mohamed MD, et al. Mutations in LCA5, encoding the ciliary protein lebercilin, cause Leber congenital amaurosis. *Nat Genet*. 2007;39:889–895.
12. Aldahmesh MA, Al-Owain M, Alqahtani F, Hazzaa S, Alkuraya FS. A null mutation in CABP4 causes Leber's congenital amaurosis-like phenotype. *Mol Vis*. 2010;16:207–212.
13. Perrault I, Hanein S, Gerard X, et al. Spectrum of SPATA7 mutations in Leber congenital amaurosis and delineation of the associated phenotype. *Hum Mutat*. 2010;31:E1241–E1250.
14. Mataftsi A, Schorderet DF, Chachoua L, et al. Novel TULP1 mutation causing leber congenital amaurosis or early onset retinal degeneration. *Invest Ophthalmol Vis Sci*. 2007;48:5160–5167.
15. Thiadens AA, den Hollander AI, Roosing S, et al. Homozygosity mapping reveals PDE6C mutations in patients with early-onset cone photoreceptor disorders. *Am J Hum Genet*. 2009;85:240–247.
16. Sergouniotis PI, Davidson AE, Mackay DS, et al. Recessive mutations in KCNJ13, encoding an inwardly rectifying potassium channel subunit, cause Leber congenital amaurosis. *Am J Hum Genet*. 2011;89:183–190.
17. Estrada-Cuzcano A, Koenekoop RK, Coppieters F, et al. IQCB1 mutations in patients with leber congenital amaurosis. *Invest Ophthalmol Vis Sci*. 2011;52:834–839.
18. Bowne SJ, Sullivan LS, Mortimer SE, et al. Spectrum and frequency of mutations in IMPDH1 associated with autosomal dominant retinitis pigmentosa and leber congenital amaurosis. *Invest Ophthalmol Vis Sci*. 2006;47:34–42.
19. Wang X, Wang H, Cao M, et al. Whole-exome sequencing identifies ALMS1, IQCB1, CNGA3, and MYO7A mutations in patients with Leber congenital amaurosis. *Hum Mutat*. 2011;32:1450–1459.
20. Peshenko IV, Olshevskaya EV, Azadi S, Molday LL, Molday RS, Dizhoor AM. Retinal Degeneration 3 (RD3) Protein inhibits catalytic activity of retinal membrane guanylyl cyclase (RetGC) and its stimulation by activating proteins. *Biochemistry*. 2011;50:9511–9519.
21. Lorenz B, Poliakov E, Schambeck M, Friedburg C, Preising MN, Redmond TM. A comprehensive clinical and biochemical functional study of a novel RPE65 hypomorphic mutation. *Invest Ophthalmol Vis Sci*. 2008;49:5235–5242.
22. Marmor MF, Zrenner E. International Society for Clinical Electrophysiology of Vision. Standard for clinical electroretinography (1999 update). *Doc Ophthalmol*. 1998;97:143–156.
23. Lorenz B, Wabbels B, Wegscheider E, Hamel CP, Drexler W, Preising MN. Lack of fundus autofluorescence to 488 nanometers from childhood on in patients with early-onset severe retinal dystrophy associated with mutations in RPE65. *Ophthalmology*. 2004;111:1585–1594.
24. Rüschendorf F, Nürnberg P. ALOHOMORA: a tool for linkage analysis using 10K SNP array data. *Bioinformatics*. 2005;21:2123–2125.

25. Abecasis GR, Cherny SS, Cookson WO, Cardon LR. Merlin—rapid analysis of dense genetic maps using sparse gene flow trees. *Nat Genet*. 2002;30:97–101.
26. Chang B, Heckenlively JR, Hawes NL, Roderick TH. New mouse primary retinal degeneration (rd-3). *Genomics*. 1993; 16:45–49.
27. Hawes NL, Smith RS, Chang B, Davisson M, Heckenlively JR, John SW. Mouse fundus photography and angiography: a catalogue of normal and mutant phenotypes. *Mol Vis*. 1999;5: 22.
28. Woodford BJ, Liu Y, Fletcher RT, et al. Cyclic nucleotide metabolism in inherited retinopathy in collies: a biochemical and histochemical study. *Exp Eye Res*. 1982;34:703–714.
29. Acland GM, Fletcher RT, Gentleman S, Chader GJ, Aguirre GD. Non-allelism of three genes (rcd1, rcd2 and erd) for early-onset hereditary retinal degeneration. *Exp Eye Res*. 1989;49:983–998.
30. Kukekova AV, Goldstein O, Johnson JL, et al. Canine RD3 mutation establishes rod-cone dysplasia type 2 (rcd2) as ortholog of human and murine rd3. *Mamm Genome*. 2009;20: 109–123.
31. Santos-Anderson RM, Tso MO, Wolf ED. An inherited retinopathy in collies. A light and electron microscopic study. *Invest Ophthalmol Vis Sci*. 1980;19:1281–1294.
32. Tomita H, Sugano E, Yawo H, et al. Restoration of visual response in aged dystrophic RCS rats using AAV-mediated channelopsin-2 gene transfer. *Invest Ophthalmol Vis Sci*. 2007;48:3821–3826.
33. Ivanova E, Hwang GS, Pan ZH, Troilo D. Evaluation of AAV-mediated expression of Chop2-GFP in the marmoset retina. *Invest Ophthalmol Vis Sci*. 2010;51:5288–5296.
34. Doroudchi MM, Greenberg KP, Liu J, et al. Virally delivered channelrhodopsin-2 safely and effectively restores visual function in multiple mouse models of blindness. *Mol Ther*. 2011;19:1220–1229.
35. Azadi S, Molday LL, Molday RS. RD3, the protein associated with Leber congenital amaurosis type 12, is required for guanylate cyclase trafficking in photoreceptor cells. *Proc Natl Acad Sci U S A*. 2010;107:21158–21163.
36. Lavorgna G, Lestingi M, Ziviello C, et al. Identification and characterization of C1orf36, a transcript highly expressed in photoreceptor cells, and mutation analysis in retinitis pigmentosa. *Biochem Biophys Res Commun*. 2003;308:414–421.
37. Li Y, Wang H, Peng J, et al. Mutation survey of known LCA genes and loci in the Saudi Arabian population. *Invest Ophthalmol Vis Sci*. 2009;50:1336–1343.
38. Schulze-Bonsel K, Feltgen N, Burau H, Hansen L, Bach M. Visual acuities "hand motion" and "counting fingers" can be quantified with the Freiburg Visual Acuity Test. *Invest Ophthalmol Vis Sci*. 2006;47:1236–1240.